On the time scale associated with Monte Carlo simulations

Reference:
Bal Kristof, Neyts Erik.- *On the time scale associated with Monte Carlo simulations*
The journal of chemical physics - ISSN 0021-9606 - 141(2014), 204104
DOI: http://dx.doi.org/doi:10.1063/1.4902136

On the time scale associated with Monte Carlo simulations

Kristof M. Bal* and Erik C. Neyts

University of Antwerp, Research Group PLASMANT, Department of Chemistry,

Universiteitsplein 1, 2610 Wilrijk, Antwerp, Belgium

Abstract

Uniform-acceptance force-bias Monte Carlo (fbMC) methods have been shown to be a powerful technique to access longer timescales in atomistic simulations allowing, for example, phase transitions and growth. Recently, a new fbMC method, the time-stamped force-bias Monte Carlo (tfMC) method, was derived with inclusion of an estimated effective timescale; this timescale, however, does not seem able to explain some of the successes the method. In this contribution we therefore explicitly quantify the effective timescale tfMC is able to access for a variety of systems, namely a simple single-particle, one-dimensional model system, the Lennard-Jones liquid, an adatom on the Cu(100) surface, a silicon crystal with point defects and a highly defected graphene sheet, in order to gain new insights in the mechanisms by which tfMC operates. It is found that considerable boosts, up to three orders of magnitude compared to molecular dynamics, can be achieved for solid state systems by lowering of the apparent activation barrier of occurring processes, while not requiring any system-specific input or modifications of the method. We furthermore address the pitfalls of using the method as a replacement or complement of molecular dynamics simulations, its ability to explicitly describe correct dynamics and reaction mechanisms, and the association of timescales to MC simulations in general.

* Corresponding author, e-mail: kristof.bal@uantwerpen.be

I. Introduction

Molecular dynamics (MD) simulations have been shown to be an invaluable tool to investigate both static and dynamic properties of systems at the atomic scale. MD simulations are a robust and versatile technique and allow tracing the full dynamical path of the system through space and time. However, many processes take place at timescales well beyond the reach of pure MD simulations, which are typically limited to the pico- or nanosecond range. Several so-called accelerated molecular dynamics methods[1,2] were therefore developed by Voter and co-workers in order to extend the MD timescale. Although these methods allow to speed up of MD simulations by several orders of magnitude, they are also limited to infrequent event systems, in which the system evolves through infrequent transitions from one metastable state to another. Many systems, however, violate this assumption. For instance, bond-switching events in the Ni/C system have been shown to occur at the sub-ps timescale, although the actual nickel-catalyzed growth of carbon nanotubes exceeds the timescale limits of MD.[3]

A different and potentially more general way to access longer timescales in atomistic simulations is the coupling of MD simulations with stochastic Monte Carlo (MC) simulations.[4] In this joint approach, an MD cycle can used to simulate fast processes (e.g. impacts on a surface), while the subsequent MC steps take into account the longer timescale thermal relaxation processes. Because the Metropolis Monte Carlo (MMC) method[5] was originally developed to carry out efficient sampling of the configuration space, it can be expected that it is able to efficiently relax an out-of-equilibrium system. Indeed, it has been shown that the sequential application of MD and MMC allows an enhanced description of thin film growth, as evidenced by the higher quality of the obtained films that better match experimental results.[6-9] This comes at the cost of losing detailed information on the described physical timescale, of which only rough estimates are available.[8]

Kikuchi et al.[10,11] furthermore showed that MMC can be interpreted as a numerical solution of the Fokker-Planck equation and thus in principle has the ability to describe the true time evolution of Brownian diffusion processes. Because the MC system evolution corresponds to actual physical events, an MC step can thus be considered to be proportional to an MD time step. The size of this (statistical) MC time step has been explicitly determined in the case of diffusion in liquids by comparing the respective diffusivity in MD and MC simulations,[12,13] whereas explicit formulas were derived in the case of colloidal particles.[14-18]

In order to increase the MC acceptance rate in strongly interacting systems, the force-bias MC (fbMC) method[19,20] was developed. By including deterministic forces into the stochastic MC algorithm, fbMC methods have much larger acceptance ratios than conventional MMC simulations. It was later recognized that the method can even be turned into a uniform acceptance algorithm, i.e., in which each Monte Carlo step is accepted with unit probability,[21] provided that the maximum allowed particle displacement is chosen to be sufficiently small.[22] This "uniform-acceptance force-bias Monte Carlo" (UFMC) shows great potential: processes such as surface diffusion,[23] phase transitions,[23] thin film growth,[24] and the growth of carbon nanotubes[25] and graphene[26] have been successfully modeled by UFMC or a hybrid MD/UFMC approach. Indeed, (hybrid) UFMC simulations seem to describe much longer timescales than those that can be reached by conventional "pure" MD.[23,25]

The origin of the apparent efficiency of fbMC with respect to MD, however, is not immediately clear. Mees et al.[27] attempted to answer this question and, starting from the canonical ensemble, derived a new uniform acceptance force-bias MC algorithm which they dubbed "time-stamped force-bias Monte Carlo" (tfMC). A universal timescale was derived, and the authors suggested that the method could be a valuable MD alternative, which would still be able to describe system dynamics but with an enhanced timescale. Moreover, the new method was recently also successfully applied to study carbon nanotube (CNT) cap

nucleation[28] and phase transitions[29]. However, the obtained time step of about 10 fs, although an order of magnitude larger than a typical MD time step, is not nearly large enough to explain, for example, the growth of defect-free carbon nanotubes. The validation of the timescale was furthermore rather limited; in fact, all previous quantitative MC timescale studies had a small scope and only considered one particular process or system, mainly diffusion in liquids, and never bound systems undergoing chemical reactions.

In this contribution, we present an extensive study of the tfMC timescale. The aim of our work is twofold. Firstly, we will explicitly quantify the timescale tfMC is able to access for a variety of systems, ranging from a simple single-particle, one-dimensional model system to amorphous solids – which is to our knowledge the largest scope of such a "calibration" yet – in order to gauge the method's applicability for these various classes of systems. Secondly, we wish to gain further general insight in the tfMC method, the mechanisms by which it operates and how these affect its performance for all kinds of systems.

This paper is organized as follows. First, the tfMC method is reviewed and its dependence on its main parameters is investigated (Sec. II). After having described the general computational details (Sec. III), the tfMC timescale is studied for three systems in equilibrium: the Lennard-Jones liquid, an adatom on the Cu(100) surface and a silicon crystal with point defects (Sec. IV). As a last system, the healing of a highly defected graphene structure is studied as model system for defect healing in CNT growth, the as of yet most successful application of fbMC methods (Sec. V).

II. Theoretical discussion

A. Description of the tfMC method

In a single tfMC simulation step, each atom *i* is displaced over a distance $\xi_{i,j}\Delta_i$ in every Cartesian direction *j*. $\xi_{i,j}$ is a stochastic variable distributed according to[27]

$$p(\xi_{i,j}) = \begin{cases} \dfrac{e^{\gamma_{i,j}(2\xi_{i,j}+1)} - e^{-\gamma_{i,j}}}{e^{\gamma_{i,j}} - e^{-\gamma_{i,j}}} & \text{if} \quad \xi_{i,j} \in [-1,0[\\ \dfrac{e^{\gamma_{i,j}} - e^{\gamma_{i,j}(2\xi_{i,j}-1)}}{e^{\gamma_{i,j}} - e^{-\gamma_{i,j}}} & \text{if} \quad \xi_{i,j} \in]0,1] \end{cases}, \tag{1}$$

with

$$\gamma_{i,j} = \frac{F_{i,j}\Delta_i}{2k_BT}, \tag{2}$$

in which $F_{i,j}$ is the force acting on the atom along component *j*, k_B the Boltzmann constant, and *T* the temperature. The maximal displacement length of atom *i*, Δ_i, is dependent on its mass and is calculated from a system-wide parameter Δ, the atom's mass m_i, and the smallest mass in the system $m_{\min}$:

$$\Delta_i = \Delta\sqrt{\frac{m_{\min}}{m_i}}, \tag{3}$$

where Δ should be chosen to be sufficiently small in order to comply with detailed balance.[22,27] The tfMC timescale was derived by realizing that an (statistically relevant) average time step could be related to the mean displacement $\langle\delta_{i,j}\rangle$

$$\begin{aligned}\langle \delta_{i,j} \rangle &= \Delta \int_{-1}^{1} | \xi_{i,j} | \, p(\xi_{i,j}) \mathrm{d}\xi_{i,j} \\ &\approx \frac{\Delta}{3}\end{aligned}, \tag{4}$$

and velocity of the atoms

$$\langle v_{i,j} \rangle = \sqrt{\frac{2k_B T}{\pi m_i}} \ , \tag{5}$$

so that

$$\begin{aligned}\langle \Delta t \rangle &= \frac{\langle \delta_{i,j} \rangle}{\langle v_{i,j} \rangle} \\ &\approx \frac{\Delta}{3} \sqrt{\frac{\pi m_{\min}}{2k_B T}}\end{aligned} . \tag{6}$$

(6) also explains the particular form of (3), which ensures that the average tfMC time step is not mass-dependent. It can be calculated that, according to (6), the time step will be in the order of 10 fs for typical condensed matter simulations. Besides being able to describe longer timescales than MD, uniform-acceptance fbMC methods also have advantages over conventional MC methods such as MMC. Not only do they not require an explicit acceptance procedure for trial moves, but they also generate a system evolution in an MD-like fashion, in which all atoms are displaced at once in every step, instead of the single-particle moves common in MMC.

It is obvious that the choice of Δ is crucial to the success of the simulation: larger values allow for a faster system evolution but, at the same time, a larger violation of detailed balance. Indeed, the algorithm is formally only correct in the limit of an infinitesimally small Δ,[22,27] meaning that *any* practical simulation will violate detailed balance to some degree. Nevertheless, a correction could be applied to circumvent the uniform acceptance

approximation by explicitly calculating the acceptance criterion. For a simple 1D test system it was shown that for processes with barriers in the order of 0.25 eV and $\Delta = 0.1$ Å , this approach leads to rejection probabilities in the order of 10%,[22] although under these conditions the method is still found to be equivalent to MMC[22] and generates correct canonical averages, even for larger choices of Δ and interaction strength.[27] Thus, it appears that explicitly monitoring the acceptance rate of an fbMC simulation does not result in immediately available conclusions about the practical validity of the method. Rather, a careful validation of the obtained physics can be used as a more practical measure of the safe range of Δ. For example, Timonova et al. carried out an extensive validation of UFMC for the study of processes in silicon, and found that values of Δ up to 0.25 Å lead to results equivalent to MD simulations.[23] Studies of carbon nanotube growth[25] and Cu adatom diffusion[27] also confirmed that maximum displacement lengths between 0.1 and 0.15 Å (about 5-10% of a typical nearest neighbor distance) lead to physically meaningful results, in agreement with either MD simulations or the experiment, and can be considered "conservative" choices.

B. Importance of Δ

It is important to note the linear relation between Δ and $\langle \Delta t \rangle$, as this contradicts the idea of an MC simulation being a random walk. Indeed, it has been recognized by many authors[14-18] that an (M)MC timescale should be proportional to the squared MC displacement length. Although these previous results were only obtained for MMC and Brownian systems (i.e. liquids), their basic principles should still be applicable to tfMC simulations of bound systems.

To elucidate this contradiction, we consider a simple one-dimensional case study: diffusion of a single particle in the sinusoidal potential surface $U(x)$:

$$U(x) = \frac{Q}{2}\left[1 - \cos\left(\frac{2\pi x}{L}\right)\right], \tag{7}$$

in which Q and L are the energy barrier and the period of the potential, respectively. If we assume that the number of jumps over the barrier is proportional to the physical time described by the simulation, such a simple model system will allow us to gain a fundamental insight into tfMC simulations of bonded systems. Indeed, other studies[22,23,27] of UFMC and tfMC have already used this model system and, for example, have found that tfMC is able to generate the correct canonical distribution.[27]

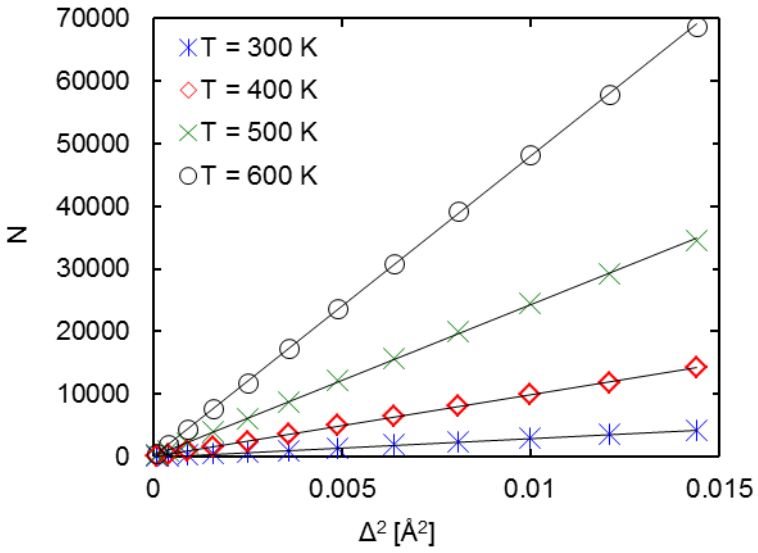

Figure 1: Dependence of the number of effective transitions N, and hence time, on the maximal displacement squared Δ^2, for various temperatures, during 10^9 tfMC iterations. Q was taken to be 0.25 eV, $L = 1$ Å.

In this study, we first performed a series of simulations at various temperatures, in which we checked the influence of the maximum displacement length Δ. Q was taken to be 0.25 eV, $L = 1$ Å, and each simulation consisted of 10^9 iterations in order to gain sufficient statistics, during which the number of jumps N was counted by only considering minimum-to-minimum transitions ("effective" transitions). It is clear from Figure 1 that the tfMC

timescale, based on the number of effective transitions, indeed is proportional to Δ^2, as is the case for other MC timescales. As mentioned earlier, this can be understood by seeing the tfMC simulation as conducting a random walk: each subsequent step is independent of the previous simulation steps. The timescale described by (6), however, assumes that the tfMC trajectory can be mapped onto an MD-like trajectory in which all steps are inherently correlated, contributing to one smooth trajectory. This assumption is closely tied to the suggestion of the tfMC authors that the method would be able to describe (approximate) system dynamics, which however cannot be achieved by a random walk.

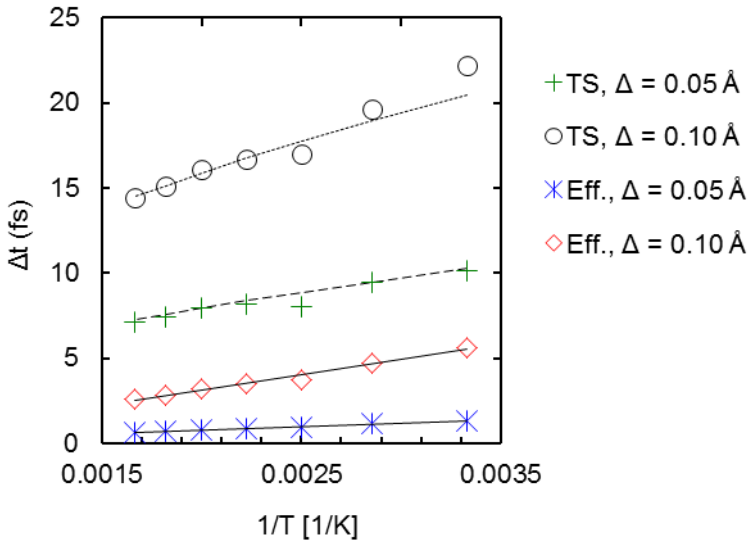

Figure 2: Time step size of an individual tfMC step, calculated for $\Delta = 0.05$ and 0.1 Å using both effective transitions or TS crossings. Dashed lines are corresponding time steps as calculated using (6), whereas solid lines are least squares fitted straight lines. *Q* was taken to be 0.25 eV, $L = 1$ Å.

In order to explicitly quantify the "real" tfMC timescale, rather than only establishing qualitative relations, we compared the number of effective transitions with those in an MD simulation (using a time step of 1 fs, 10^9 steps per run, velocity Verlet integration[30] and an

Andersen thermostat[31] with a collison time of 1 ps), in which the tfMC time step is measured as

$$\langle \Delta t \rangle_{\mathrm{tfMC}} = \Delta t_{\mathrm{MD}} \frac{N_{\mathrm{tfMC}}}{N_{\mathrm{MD}}} \ , \tag{8}$$

and N the number of transitions. Figure 2 clearly shows that the tfMC timescale (6) overestimates the real, physical time when one is interested in actual, effective transitions and which only is about 1 to 5 fs. What the figure also shows, however, is that the tfMC timescale is correct as long one only considers processes occurring in a single tfMC step. Indeed, while an effective (minimum-to-minimum) transition is not such a single-step process, but the crossing of the transition state (TS) is. The difference between real dynamics and tfMC trajectories is that, according to transition state theory (TST), every effective transition coincides with a single TS crossing, whereas due to the random walk-like nature of tfMC, many TS (re)crossings can happen in the course of only one effective transition (or the system may even end up in the original minimum again).

C. Effect of the temperature

It has been suggested by both Timonova et al.[23] and Neyts et al.[22] that fbMC methods are able to capture system dynamics because they are able to "feel" reaction barriers. When carrying out simulations using the sinusoidal potential (7), they noted that an Arrhenius plot could be used to obtain the activation energy Q of the diffusion process,

$$\ln(N) = \ln(\nu_0 t) - \frac{Q}{k_B T} \ , \tag{9}$$

implying that temperature-dependent dynamics could be reproduced using fbMC simulations. It was also found, however, that the "measured" activation energy was always lower than the imposed value Q, which inspired the hypothesis that this lowering of the apparent activation

energy is the mechanism by which fbMC methods operate,[22,23] as this can lead to significant speed-ups of the simulation compared to MD.

As has been noted in the previous section, however, it is dangerous to assume MC methods can be treated as if they were MD. In particular, it should be established whether the tfMC timescale is temperature-dependent: (6) already suggests it is, although this relation provides an incorrect estimate of the tfMC time step. Still, intuitively one expects there should be a temperature effect: Δ imposes a limit on the displacement length per iteration and is temperature-independent, whereas in an MD simulation, atoms will be able to travel a longer distance per time step at higher temperatures.

A qualitative derivation, suited for solid state systems, is as follows. Although it is not possible to map a single tfMC step to an MD step, atomic movement is most of the time also limited by a maximum displacement length: the vibrational amplitude A of the atom in a potential energy well. Assuming this well is harmonic and has an associated force constant k_f, the equipartition theorem then states that $k_f A^2 = 2k_B T$. Recognizing that the tfMC timescale is proportional to Δ^2, which can be seen as equivalent to A^2, one finds

$$t \sim \frac{k_f \Delta^2}{T} \ . \tag{10}$$

When inspecting Figure 2, one clearly sees that it indeed recovers this 1/T dependence of the tfMC timescale.

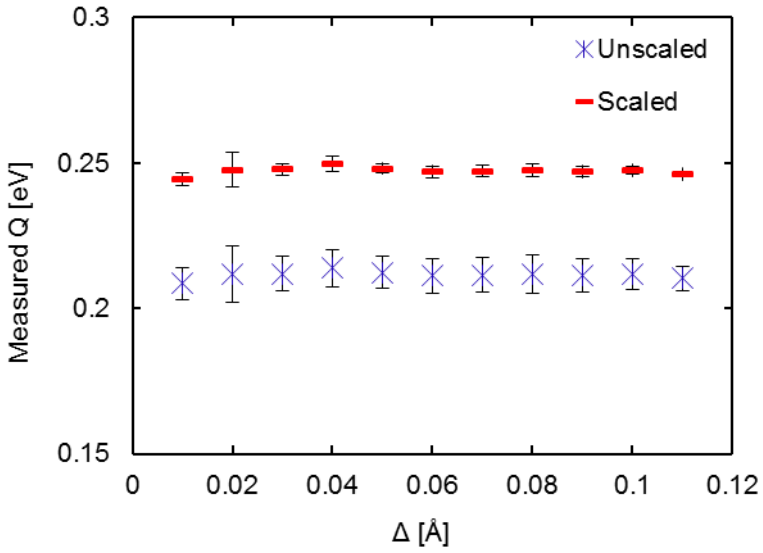

Figure 3: Measured activation energies Q, using either an unscaled or a scaled Arrhenius fit, for different choices of Δ. Set value of Q is 0.25 eV, $L = 1$ Å.

This also means one has to compensate for this fact when calculate activation barriers through an Arrhenius fit: Figure 3 demonstrates this, by showing both the measured values of Q when directly using a plot of $\ln(N)$ vs. $1/T$ or by compensating for the T-dependence by using $\ln(N \cdot T)$ instead. The first method clearly underestimates the imposed value of $Q = 0.25$ eV by about 20%, in agreement with previous results,[22] whereas the compensated variant recovers the correct value (a small underestimation of about 2% remains, probably due to the coarser nature of the tfMC steps). Also, it can be seen that the unscaled approach yields much larger uncertainties (at the 95% confidence level) on the calculated barriers as a result of the poorer fit. This is an encouraging result as it shows that tfMC simulation do resemble actual dynamical simulations under certain conditions, even with mechanisms that are very close to the actual, physical dynamics. Moreover, although the enhancement compared to MD is not as large as the original timescale (6) suggests, tfMC indeed is able to describe longer timescales then MD. These time step values of 1 to 5 fs are, however, not

large enough to explain the method's successes describing growth and phase transitions, a question we will address in the following sections.

III. General computational methodology

For all following simulations, the LAMMPS package[32] was used. NVT MD simulations were performed using a Nosé-Hoover chain thermostat[33] (three thermostats), whose equations of motion were integrated using the algorithm of Martyna et al.[34] as implemented in LAMMPS. Prior to this production stage, the system was always equilibrated with a Langevin-type thermostat[35] in combination with velocity Verlet integration.[30] Damping constants for the thermostats were always set to be equal to $100\Delta t_{\mathrm{MD}}$ and periodic boundaries were used in all directions. For this study, the tfMC method was implemented in LAMMPS as an additional fix[36] and the method was used for both production runs as the preceding equilibration.

IV. Systems in equilibrium

A. Determination of the timescale

In this section we will explicitly quantify the tfMC timescale for various different systems in equilibrium. In such systems, no specific transition from one macrostate to another can occur so that their transport properties provide a simple and constant benchmark. A tfMC time step $\langle \Delta t \rangle_{\mathrm{tfMC}}$ can be estimated by comparing a selected property, e.g., a mean square displacement (MSD) with the same property as obtained from an MD simulation of the same number of steps and with time step Δt_{MD}:

$$\langle \Delta t \rangle_{\mathrm{tfMC}} = \Delta t_{\mathrm{MD}} \frac{\mathrm{MSD}_{\mathrm{tfMC}}}{\mathrm{MSD}_{\mathrm{MD}}} \ . \tag{11}$$

B. The Lennard-Jones liquid

As the simplest of systems, the Lennard-Jones liquid is an attractive model system to study liquid diffusion and offers a simple method of calibrating the tfMC timescale. Throughout this section, reduced units are used. In all simulations, the system consisted of 4000 atoms in a cubic periodic box, with a density of $\rho^* = 0.9$ and at a temperature of $T^* = 1$. The MD time step was 0.005, whereas various values of Δ were used in order to verify the scaling of the tfMC time step size. In order to establish the safe range of Δ values, we monitored the potential energy and radial distribution functions of the system, and found that for values of $\Delta = 0.14$ and below, no anomalous energy fluctuations and incorrect radial distribution functions were obtained.[36] The system was allowed to equilibrate for 10^6 steps, after which the MSD was obtained during a production run of the same length. For each value of Δ, the time content of a tfMC step was calculated using (11).

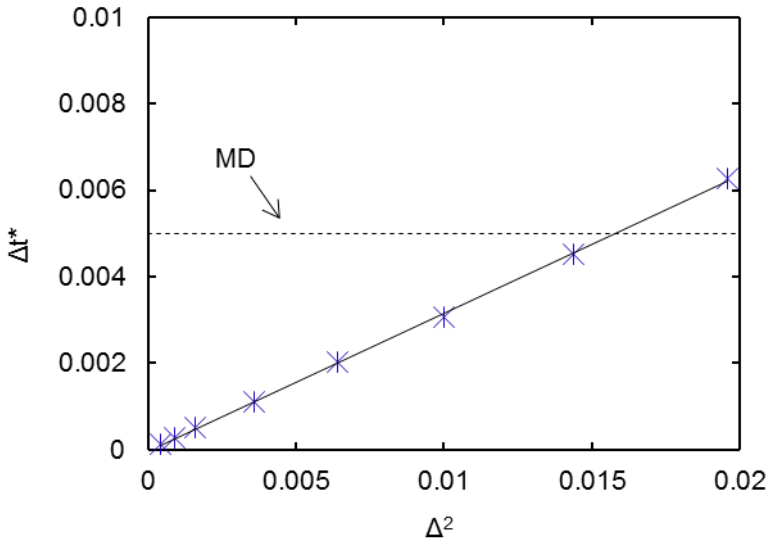

Figure 4: Magnitude of the tfMC time step and its dependence the size of Δ^2, as obtained through comparison with MD, for the LJ liquid. The magnitude of the MD time step (0.005 a.u.) is also shown for clarity.

It is clear from Figure 4 that the $t \sim \Delta^2$ scaling also holds for this real system, in agreement with previous MMC studies. It is also seen that tfMC, within its safe range, is hardly competitive with MD in terms of the described timescale. Indeed, tfMC only surpasses MD for $\Delta \approx 0.12$, very close to the $\Delta = 0.14$ limit. The original tfMC timescale, however, predicts a much larger tfMC time step: for $\Delta = 0.1$, one finds a time step of about 0.04, whereas the actual value (through the MSD) is only 0.003. This further confirms that the "universal" tfMC timescale is not correct. The specific observation that tfMC performs poorly in simulating liquid diffusion is in fact a general aspect of stochastic methods. Not only MC, but also stochastic MD techniques such as the Andersen or Langevin thermostats do not conserve (or, in the case of MC, possess) momentum; liquid diffusion, however, is driven by momentum transport. Indeed, when Huitema and van der Eerden[12] performed a similar MSD-based calibration of the MMC timescale for LJ diffusion they also found their MC moves had similar time contents as a single MD step, and furthermore pointed out that using a formula such as (6) to determine the MC time step would be "naive".

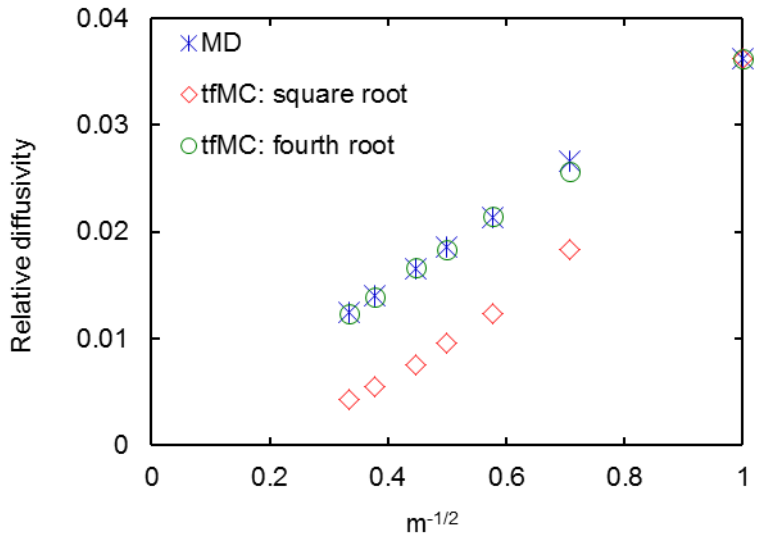

Figure 5: Effect of the mass-based scaling of Δ_i on the diffusivity calculated by tfMC. The tfMC results were rescaled to be equal to the MD result for $m = 1$.

Furthermore, it should be mentioned that a mass-based scaling of the maximal displacement length as proposed by Mees et al.[27] [equation (3)] should be modified to comply with our new findings: diffusion coefficients and reaction rate coefficients scale as $m^{-1/2}$ and hence Δ_i should be scaled as

$$\Delta_i = \Delta\left(\frac{m_{\min}}{m_i}\right)^{1/4}. \tag{12}$$

Figure 5 confirms this finding for the LJ liquid, as it shows that a tfMC simulation using our new scaling matches the mass-dependence of the MD result, whereas the original scaling does not. Using this scaling, combined with the findings in Sec. II, it can be expected that the method will be able to generate a correct pseudodynamics of mixed-element systems.

C. Surface diffusion

Although tfMC does not perform well while studying liquid diffusion, it has to be kept in mind that the method was primarily developed to be applied to bonded systems. Diffusion of adatoms on a surface constitutes an interesting model system for the study of diffusion in solid state systems, and is also well documented.[37] The simulated system consisted of an adatom on a copper(100) surface made from six consecutive layers, each containing 60 atoms. The four bottom layers were kept fixed to mimic the bulk of the crystal. The Cu-Cu interaction was described by an embedded atom (EAM) potential.[38,39] The MD time step was 1 fs and $\Delta = 0.1$ Å, using an equilibration stage of 10^5 steps and a production run of 10^8 steps, collecting data within a temperature range between 500 and 800 K. The tfMC timescale was determined using (11), but instead of the MSD, the number of adatom hops *N* was used.

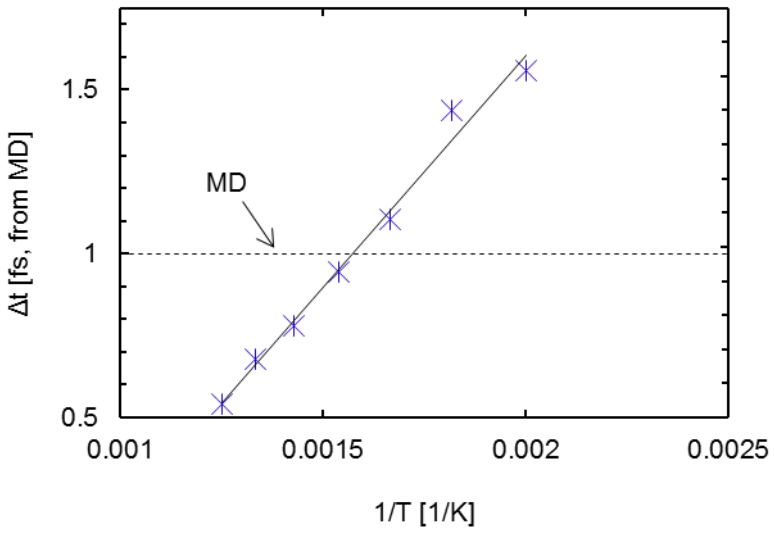

Figure 6: Magnitude of the tfMC time step and its dependence on the inverse temperature $1/T$ for $\Delta = 0.1$ Å, as obtained through comparison with MD, for adatom diffusion on Cu(100). The magnitude of the MD time step (1 fs) is also shown for clarity.

It is clear from Figure 6 that the temperature dependence of the tfMC timescale follows a $1/T$ relation, in agreement with our earlier findings. Furthermore, it can be seen that for a conservative step size of $\Delta = 0.1$ Å, tfMC is competitive with MD, although the corresponding time step of about 1 fs does not constitute a real improvement over MD. In order to gauge the method's accuracy in reproducing dynamical properties, we calculated the (apparent) activation energy for an adatom hop through an Arrhenius fit. Our MD result is 0.52 ± 0.02 eV, in agreement with other studies using the same potential.[40-43] An Arrhenius fit of the tfMC results without temperature correction (i.e., using $\ln(N)$ rather than $\ln(N \cdot T)$) unsurprisingly yields an activation energy of 0.41 ± 0.02 eV, which is much too low. This observation was also made by Timonova et al.[23] during the UFMC study of surface diffusion, but, as they obtained a similar activation energy lowering for the sinusoidal potential (7), attributed it to some inherent property of the method. However, when compensating for the temperature dependence of the tfMC timescale in a similar fashion as we did earlier for the

sinusoidal potential, the tfMC method yields an activation barrier of 0.46 ± 0.02 eV, much closer to the MD value and literature results of this potential.

Nonetheless, the system still experiences a somewhat smaller activation energy in tfMC simulations than in MD. Thus, although the global dynamical behavior of a system in a tfMC simulation will be very similar to the "real" dynamics, small discrepancies might still occur. In particular when studying more complex phenomena such as material growth, different processes can occur; in order to describe correct global dynamics, all the respective activation energies should be reproduced faithfully. Therefore the next section will describe a system for which we study two different processes.

D. Silicon self-diffusion

Diffusion in silicon is of great technological importance considering its role in the fabrication of silicon-based integrated circuits. The simplest of these diffusion mechanisms are the two pathways of silicon self-diffusion, which can happen through either a vacancy or an interstitial mechanism. These two processes have different rate constants (with both different activation barriers and pre-exponential factors) and thus pose an interesting test case to determine the correctness of the dynamical behavior of the tfMC method. We employed a silicon crystal containing 512 ± 1 atoms with a lattice constant of 5.431 Å, modeled with the Stillinger-Weber (SW) potential.[44] The MD time step was 1 fs, whereas multiple values of Δ were used. The MSD was calculated in a temperature range between 500 and 1200 K during 10^8 steps, preceded by an equilibration run of 10^5 steps.

When using $\Delta = 0.1$ Å, a conservatively small choice for this parameter, we obtained activation energies of 0.41 ± 0.01 eV for vacancy and 0.78 ± 0.05 eV for interstitial diffusion, matching the MD results of 0.44 ± 0.02 eV and 0.86 ± 0.07 eV, respectively, and in good agreement with other simulations using the SW potential.[45-47] (We compensated for the

$t \sim T^{-1}$ scaling of the timescale in the Arrhenius fit.) By comparing the fitted pre-exponential factors of both defect types, tfMC time step sizes of 1.2 ± 0.5 and 0.74 ± 0.84 fs are found for vacancy and interstitial diffusion, respectively (the large error margins are due to exponentiation; the obtained time steps of ~1 fs were corroborated by comparing individual MSD's rather than fitted pre-exponential factors). Therefore, it can be concluded that both processes are described by tfMC with the correct relative rates, albeit without a speedup compared to MD.

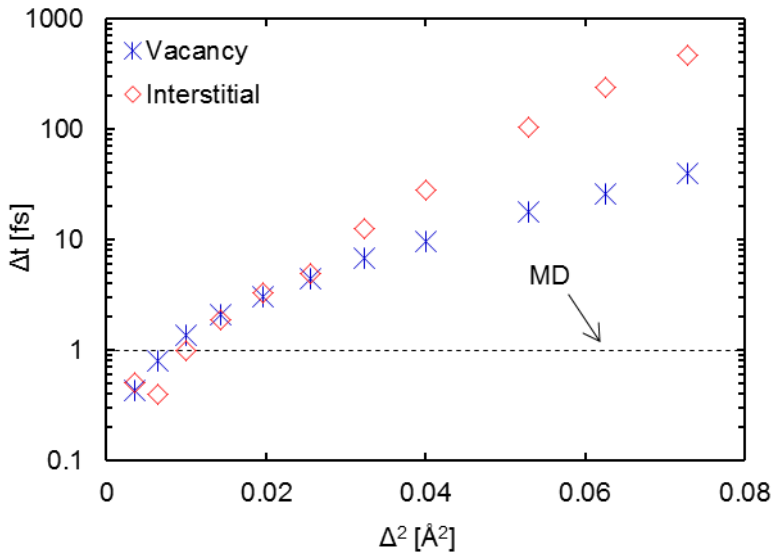

Figure 7: Magnitude of the tfMC time step, as obtained through comparison with MD, for the two diffusion pathways in silicon, at 800 K. The magnitude of the MD time step (1 fs) is also shown for clarity.

It was shown by Timonova et al., however, that UFMC is able to accomplish much higher boosts for Si-based systems, up to several orders of magnitude, provided that larger values for Δ are chosen. Indeed, as Figure 7 shows, we also observe that tfMC can possess average time steps of up to about 500 fs in the case of $\Delta = 0.27$ Å. This, however, comes at the cost of (1) incorrect relative dynamics, as interstitial diffusion is more strongly boosted than vacancy diffusion by an order of magnitude, and (2) loss of the $t \sim \Delta^2$ scaling in favor of an

exponential dependence on Δ^2. For smaller displacements ($\Delta < 0.1$ Å) on the other hand, we also verified and recovered this previously derived relation.

The nature of the exponential boost caused by larger Δ becomes clear when inspecting Figure 8, showing that the apparent activation energy of both processes decreases as a linear function of Δ^2. This contradicts our findings in Sec. II, were we found that tfMC reproduces the correct barriers, irrespective of the size of Δ. The main difference between the crystal currently under consideration and the model system (7) we used previously is the nature of the potential energy surface (PES). Indeed, whereas the sinusoidal potential constitutes a fixed PES for the diffusion particle, each atom in a multi-particle system is subjected to a variable PES, which is imposed by its neighbors. Larger values of Δ introduce a stronger deformation of the crystal structure, and therefore increase of the total potential energy. Assuming harmonic behavior over smaller distortions it is logical this increase of the potential energy, and subsequent lowering of apparent barriers, will have a Δ^2 dependence.

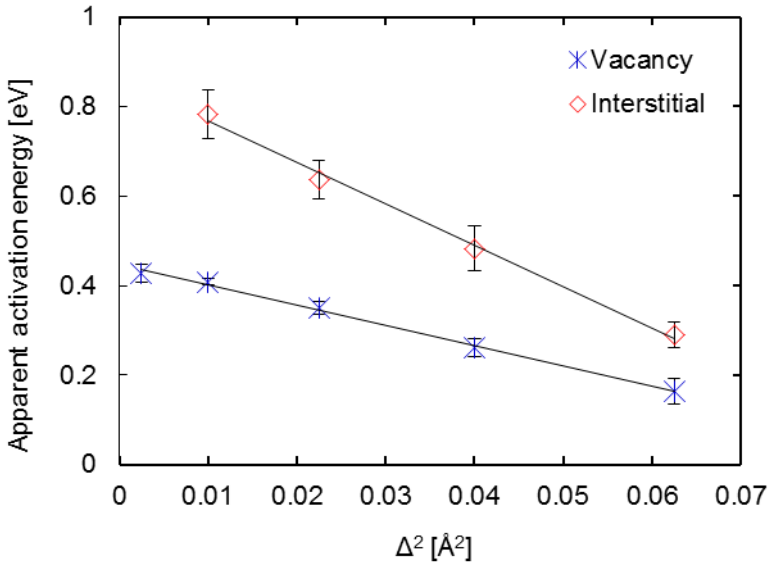

Figure 8: Apparent activation energy of the two diffusion pathways in silicon in a tfMC simulation, and its dependence on Δ^2.

Lowering of the apparent activation energy of course allows for a substantial boost, but comes at the price of losing correct relative (pseudo)dynamics: as Figure 8 shows, the apparent activation energy decreases more rapidly with increasing displacement length in case of the interstitial mechanism, possibly because its higher true barrier will be more prone to large fluctuation caused by the stochastic displacements of the diffusing atom's neighbors. Interestingly, taking the $\Delta^2 \to 0$ limit for both mechanisms recovers values in excellent agreement with MD result, i.e., 0.45 ± 0.02 and 0.86 ± 0.07 eV for the vacancies and interstitials, respectively. Thus, in the limit of an infinitesimally small maximum displacement length, one will obtain fully "correct" dynamics (and full compliance with detailed balance) but of course no advantage to MD at all. On the other hand, although large choices of Δ must certainly violate detailed balance to a certain degree, Timonova et al. found that UFMC simulations with $\Delta < 0.25$ Å are a safe choice for most processes in Si, meaning that these simulations yield a global system evolution that is still physical. It is, however, intrinsically impossible to assign a single "timescale" to such a process, as we have seen that individual processes are boosted differently.

V. Defected graphene

The most impressive application of fbMC methods has been the growth of carbon nanostructures: in the case of carbon nanotube (CNT) growth, they were instrumental in achieving the first simulations of chiral growth,[25] and nucleation from hydrocarbon precursors.[28] The crucial long-timescale process that fbMC methods (but also MMC[49,50]) allow to access is the healing of topological defects in the growing structure, in order to obtain a perfect hexagonal lattice. It is therefore interesting to quantify the tfMC timescale for a system that is closely related to these carbon-based systems as it gives an indication on the actual speed-up that was gained in the aforementioned simulations, information that is as of

yet still unavailable. In addition to the relevance of its associated timescale as such, defected graphene is also an out-of-equilibrium system and able to undergo a phase transition, which is an important class of dynamic processes this paper has not addressed up to this point.

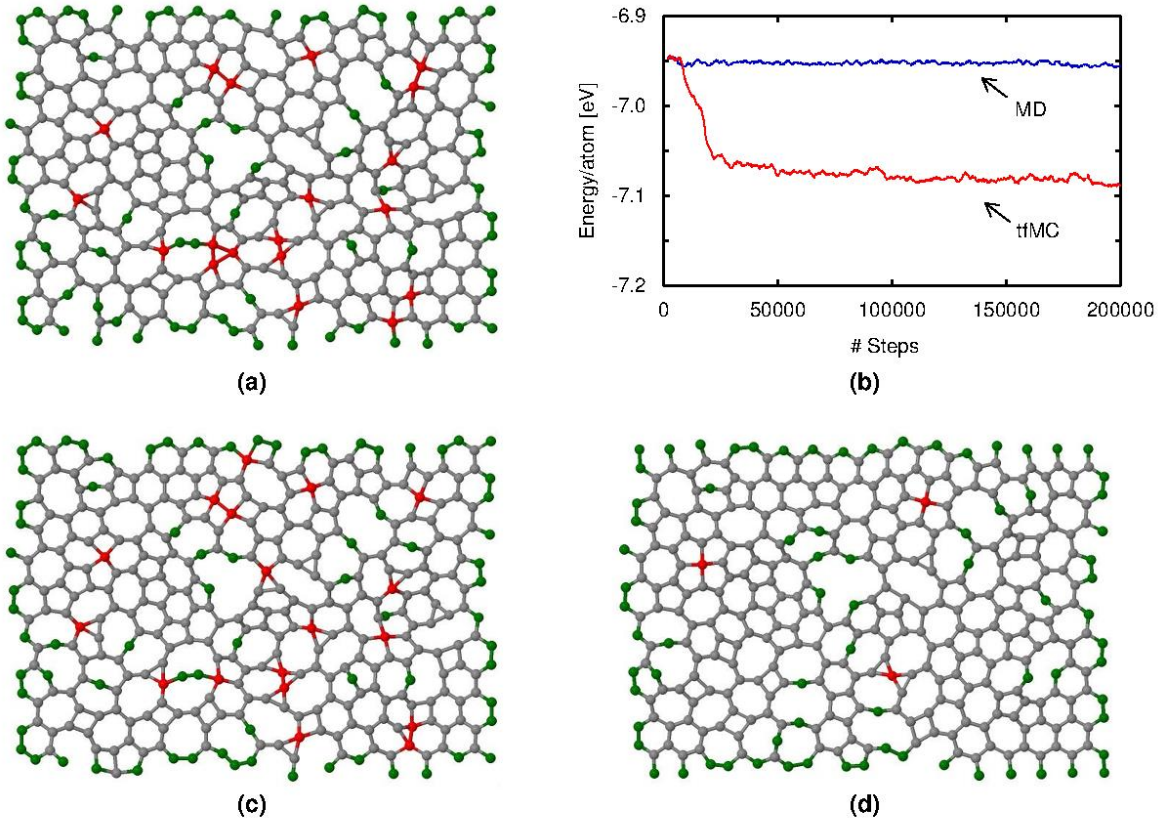

Figure 9: Healing of a defected graphene sheet. (a) Initial (equilibrated) structure; (b) evolution of the potential energy during the relaxation at 1000 K; (c) final structure after 2×10^5 MD steps; (d) final structure after 2×10^5 tfMC steps with $\Delta = 0.1$ Å. Red-colored carbon atoms are over-coordinated (higher than sp^2), green-colored are under-coordinated (lower than sp^2), respectively.

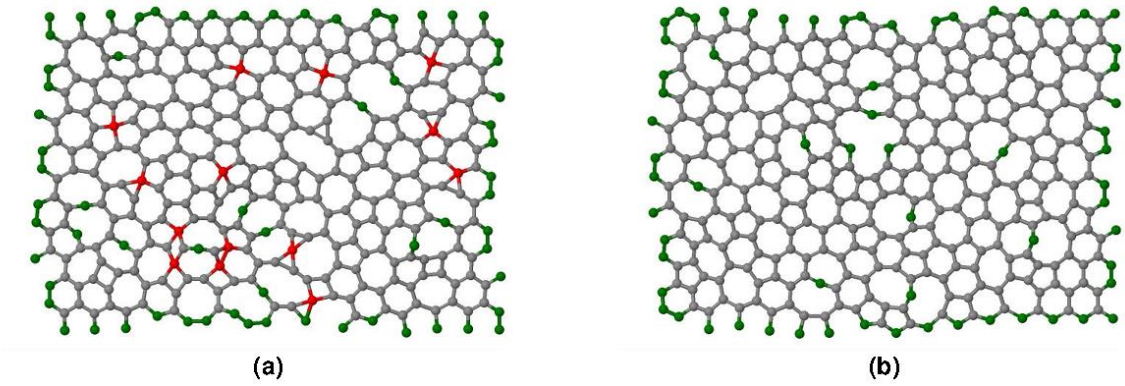

Figure 10: Further healing of the defected graphene sheet of Figure 9a, after 4×10^7 steps of (a) MD or (b) tfMC, at 1000 K. Color coding is the same as in Figure 9.

An amorphous graphene-like structure was generated by random displacement of all atoms in a perfect graphene lattice containing 360 atoms, and subsequent quenching and equilibration of 10^4 MD steps at 1000 K. The C-C interaction was described by the second generation REBO potential.[48] The MD time step was 0.25 fs, whereas Δ was chosen to be 0.05 and 0.1 Å, which were shown to yield physical results for this type of system.[25,28] After initial (pure MD) equilibration, the resulting structure was relaxed using either MD or tfMC. Figure 9 then clearly shows that, at 1000 K and using $\Delta = 0.1$ Å, tfMC is able to relax the defected structure much better than MD. Indeed, while 2×10^5 MD steps are not able to cause an appreciable energy decrease or healing, tfMC is able to rapidly lower the structure's energy by about 0.15 eV/atom and decrease the number of three-membered rings and over- or under-coordinated atoms. After 4×10^7 steps (10 ns in case of MD), the difference between the two structures (Figure 10) is even more apparent, with tfMC having healed out all over-coordination and three-membered rings (catalysis or higher temperatures are required to obtain perfect graphene only consisting of six-membered rings[49,50]).

This efficiency of MC methods has of course already been established, but the exact timescale at which this healing process takes place is not clear. In order to explicitly quantify

the boost tfMC achieves, we prepared 20 different structures at temperatures between 800 and 1500 K using the same procedure as above. These structures were relaxed using MD or tfMC with $\Delta = 0.05$ or 0.1 Å up till the point where an energy decrease of 0.15 eV/atom was reached. The average number of iterations required to achieve this target can again be used to determine the average size of the tfMC time step, or the boost the method can achieve. As Figure 11 then shows, this boost can be as large as 800 (a tfMC time step of about 200 fs) at 800 K when using $\Delta = 0.1$ Å. This boost rapidly decreases at higher temperatures to about 40 at 1500 K, but this corresponds to a tfMC time step of 10 fs, which is still substantial. The performance of the method when $\Delta = 0.05$ Å is much lower, however, as it is clear that at 800 K, it is about 300 times slower (time step of only ~0.5 fs). These huge difference between the two choices of the displacement length, combined with the rapid deterioration of the boost with increasing temperature, show that lowering of apparent activation energies also for this system plays an important role.

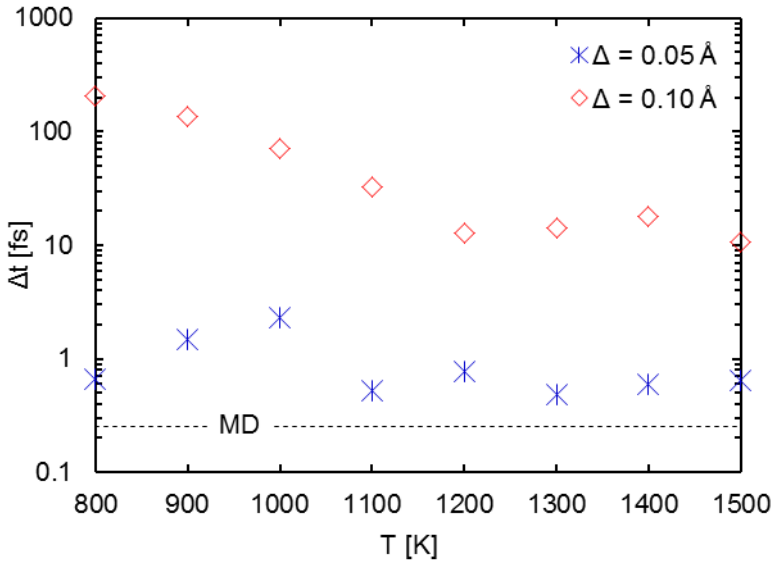

Figure 11: Magnitude of the tfMC time step, as obtained through comparison with MD, during healing of defected graphene at various temperatures, for $\Delta = 0.05$ or 0.1 Å. The magnitude of the MD time step (0.25 fs) is also shown for clarity.

The additional energy that the tfMC methods injects into the structure in the case of $\Delta = 0.1$ Å thus allows for a strongly increased healing rate, leading to similar speedups as found in the previous section. In the case of $\Delta = 0.05$ Å, a time step of similar magnitude as for the Si system with $\Delta = 0.1$ Å is found, suggesting no significant changes of the apparent barriers are introduced and a more "well-behaved" pseudodynamics. Although we cannot expect the relative importance of processes as seen in the $\Delta = 0.1$ Å to match the MD result, it is clear from our results that both simulation methods lead to the same global evolution: decrease the number of three-membered rings and over- or under-coordinated atoms. Moreover, from a thermodynamic viewpoint, all methods simulating the NVT ensemble are bound to ultimately bring the system to its free energy minimum, which is a perfect graphene sheet. The previous MD/fbMC CNT growth simulations that resulted in tubes with a definable chirality[25] are an example of such a process, and demonstrate that the incorrect "dynamics" of fbMC methods with too large a displacement can still produce physically meaningful results, albeit with loss of kinetic fidelity.

VI. Conclusions

A comprehensive study of the timescale of the time-stamped force-bias Monte Carlo (tfMC) method was carried out in order to verify the method's applicability to a wide range of systems and gain insight in the fundamental mechanisms underpinning its apparent efficiency.

Using a simple one-dimensional model system, it is found that the originally derived timescale of the tfMC method, when compared to MD results, does not match the actual physical time associated with the observed events. Indeed, tfMC does not offer a large timescale elongation compared to MD for this model system. However, it is established that

tfMC simulations are subjected to the same activation barriers and hence will be able to describe a pseudoynamics that is very close to physical dynamics as accessed by MD.

When applied to solid state systems, one has to find a compromise between physical accuracy and boost. Small maximum displacement lengths Δ ensure that the processes as obtained by tfMC closely match MD results in terms of relative importance, which guarantees both methods give rise to very similar mechanism and hence the same global evolution of the system, albeit without tfMC achieving a significant boost. If Δ is made larger, however, one can observe large speedups in comparison to what is possible using MD explaining, for example, the ability of the method to describe the growth of chiral carbon nanotubes. This large boost comes at the price of losing correct relative dynamics because this acceleration is caused by a lowering of the apparent activation energy of processes due to larger deformations of the surrounding crystal. Therefore, it can be concluded that it is inherently impossible to derive a universal timescale to describe the system evolution during a tfMC simulation.

Although the tfMC method might not be generally suited to study relative dynamics, it still generates realistic system evolutions, as evidenced by the healing of defective graphene. Because these relaxing processes can be described several orders of magnitude faster than possible with MD, the tfMC method is excellently suited as an easy to implement, simple method that is able to quickly bring the system to equilibrium. The method furthermore requires no specific system-dependent information, making it an attractive alternative to more complicated accelerated MD or kinetic Monte Carlo methods, and is from a technical perspective closer to MD than MMC. However, to extend the timescale of atomistic simulations beyond the timescales reported in this paper, or with more detailed mechanistic information, accelerated MD methods will be needed. Such methods still require further development to make them more efficient and generally applicable, an ongoing field of

research of which tfMC can be a part as well: recently, the successful combination of hyperdynamics and MC methods was presented,[51,52] thus opening new exciting perspectives for further development and applications of the tfMC method.

Acknowledgements

K.M.B. is funded as PhD fellow (aspirant) of the FWO-Flanders (Fund for Scientific Research-Flanders). This work was carried out in part using the Turing HPC infrastructure at the CalcUA core facility of the Universiteit Antwerpen (UA), a division of the Flemish Supercomputer Center VSC, funded by the Hercules Foundation, the Flemish Government (department EWI) and the UA. The authors gratefully acknowledge fruitful discussions with M. J. Mees, G. Pourtois and B. J. Thijsse.

References

[1] A. F. Voter, F. Montalenti, and T. C. Germann, Annu. Rev. Mater. Res. **32**, 321 (2002).

[2] D. Perez, B. P. Uberuaga, Y. Shim, J. G. Amar, and A. F. Voter, Annu. Rep. Comput. Chem. **5**, 79 (2009).

[3] E. Neyts, Y. Shibuta, and A. Bogaerts, Chem. Phys. Lett. 488, 202 (2010).

[4] E. C. Neyts and A. Bogaerts, Theor. Chem. Acc. **132**, 1320 (2013).

[5] N. Metropolis, A. W. Rosenbluth, M. N. Rosenbluth, A. H. Teller, and E. Teller, J. Chem. Phys. **21**, 1087 (1953).

[6] M. Taguchi and S. Hamaguchi, J. Appl. Phys. **100**, 123305 (2006).

[7] M. Taguchi and S. Hamaguchi, Thin Solid Films **515**, 4879 (2007).

[8] M. Eckert, E. Neyts, and A. Bogaerts, CrystEngComm **11**, 1597 (2009).

[9] M. Eckert, V. Mortet, L. Zhang, E. Neyts, J. Verbeeck, K. Haenen, and A. Bogaerts, Chem. Mater. **23**, 1414 (2011).

[10] K. Kikuchi, M. Yoshida, T. Maekawa, and H. Watanabe, Chem. Phys. Lett. **185**, 335 (1991).

[11] K. Kikuchi, M. Yoshida, T. Maekawa, and H. Watanabe, Chem. Phys. Lett. **196**, 57 (1992).

[12] H. E. A. Huitema and J. P. van der Eerden, J. Chem. Phys. **110**, 3267 (1999).

[13] G. Rutkai and T. Kristóf, J. Chem. Phys. **132**, 104107 (2010).

[14] G. Tiana, L. Sutto, and R. A. Broglia, Physica A **380**, 241 (2007).

[15] E. Sanz and D. Marenduzzo, J. Chem. Phys. **132**, 194102 (2010).

[16] F. Romano, C. De Michele, D. Marenduzzo, and E. Sanz, J. Chem. Phys. **135**, 124106 (2011).

[17] S. Jabbari-Farouji and E. Trizac, J. Chem. Phys. **137**, 054107 (2012).

[18] A. Patti and A. Cuetos, Phys. Rev. E **86**, 011403 (2012).

[19] C. Pangali, M. Rao, and B. J. Berne, Chem. Phys. Lett. **55**, 413 (1978).

[20] M. Rao, C. Pangali, and B. J. Berne, Mol. Phys. **37**, 1773 (1979).

[21] G. Dereli, Mol. Simul. **8**, 351 (1992).

[22] E. C. Neyts, B. J. Thijsse, M. J. Mees, K. M. Bal, and G. Pourtois, J. Chem. Theory Comput. **8**, 1865 (2012).

[23] M. Timonova, J. Groenewegen, and B. J. Thijsse, Phys. Rev. B **81**, 144107 (2010).

[24] C. Grein, R. Benedek, and T. de la Rubia, Comput. Mater. Sci. **6**, 123 (1996).

[25] E. C. Neyts, Y. Shibuta, A. C. T. van Duin, and A. Bogaerts, ACS Nano **4**, 6665 (2010).

[26] E. C. Neyts, A. C. T. van Duin, and A. Bogaerts, Nanoscale **5**, 7250 (2013).

[27] M. J. Mees, G. Pourtois, E. C. Neyts, B. J. Thijsse, and A. Stesmans, Phys. Rev. B **85**, 134301 (2012).

[28] U. Khalilov, A. Bogaerts, and E. C. Neyts, Nanoscale **6**, 9206 (2014).

[29] Y. Engelmann, A. Bogaerts, and E. C. Neyts, Nanoscale **6**, 11981 (2014).

[30] W. C. Swope, H. C. Andersen, P. H. Berens, and K. R. Wilson, J. Chem. Phys. **76**, 637 (1982).

[31] H. C. Andersen, J. Chem. Phys. **72**, 2384 (1980).

[32] S. Plimpton, J. Comput. Phys. **117**, 1 (1995).

[33] G. J. Martyna, M. L. Klein, and M. Tuckerman, J. Chem. Phys. **97**, 2635 (1992).

[34] G. J. Martyna, M. E. Tuckerman, D. J. Tobias, and M. L. Klein, Mol. Phys. **87**, 1117 (1996).

[35] G. Bussi and M. Parrinello, Phys. Rev. E **75**, 056707 (2007).

[36] See supplemental material at [URL will be inserted by AIP] for additional details on our LAMMPS code and the choice of the maximal displacement in the LJ system.

[37] T. Ala-Nissila, R. Ferrando, and S. C. Ying, Adv. Phys. **51**, 949 (2002).

[38] M. S. Daw and M. I. Baskes, Phys. Rev. B **29**, 6443 (1984).

[39] S. M. Foiles, M. I. Baskes, and M. S. Daw, Phys. Rev. B **33**, 7983 (1986).

[40] G. Boisvert and L. J. Lewis, Phys. Rev. B **56**, 7643 (1997).

[41] H. Yildirim, A. Kara, S. Durukanoglu, and T. S. Rahman, Surf. Sci. **600**, 484 (2006).

[42] H. Yildirim, A. Kara, and T. S. Rahman, Phys. Rev. B **76**, 165421 (2007).

[43] L. Kong and L. J. Lewis, Phys. Rev. B **77**, 165422 (2008).

[44] F. H. Stillinger and T. A. Weber, Phys. Rev. B **31**, 5262 (1985).

[45] G. H. Gilmer, T. Diaz de la Rubia, D. M. Stock, and M. Jaraiz, Nucl. Instrum. Methods Phys. Res. B **102**, 247 (1995).

[46] K. Kakimoto, T. Umehara, and H. Ozoe, J. Cryst. Growth **210**, 54 (2000).

[47] M. Posselt, F. Gao, and H. Bracht, Phys. Rev. B **78**, 035208 (2008).

[48] D. W. Brenner, O. A. Shenderova, J. A. Harrison, S. J. Stuart, B. Ni, and S. B. Sinnott, J. Phys.: Condens. Matter **14**, 783 (2002).

[49] S. Karoui, H. Amara, C. Bichara, and F. Ducastelle, ACS Nano **4**, 6114 (2010).

[50] M. Diarra, H. Amara, C. Bichara, and F. Ducastelle, Phys. Rev. B **85**, 245446 (2012).

[51] P. Tiwary and A. van de Walle, Phys. Rev. B **84**, 100301 (2011).

[52] P. Tiwary and A. van de Walle, Phys. Rev. B **87**, 094304 (2013).